Engineered Science

RESEARCH PAPER

View Article Online

Dynamic oscillatory rheological properties of polystyrene/poly(methyl methacrylate) blends and their composites in the presence of carbon black

Yamin Pan,[1,2] Dirk W. Schubert,[2] Jong Eun Ryu,[3] Evan Wujick,[4] Chuntai Liu,[1] Changyu Shen[1] and Xianhu Liu*[1,2]

In this work, the polystyrene/poly(methyl methacrylate) ((PS/PMMA) blends and their composites with different PS/PMMA ratios and different carbon black (CB) contents were prepared by melt mixing. The rheological properties of immiscible PS/PMMA blends and PS/PMMA/CB composites are deeply discussed to understand the relationship between the rheological properties and the CB particle network. For the blends with a sea-island morphology, a shoulder is observed at low-frequency region due to the shape relaxation of dispersed droplets. However, for the blends with a co-continuous morphology, the frequency sweep exhibits power-law dependences with a small terminal slope. As the CB concentration increases, the slope of storage moduli versus angular frequency plots in the low angular frequencies becomes much lower than 1. This suggests that the composite exhibits a transformation from liquid-like to solid-like states. Moreover, a linear relationship between the storage moduli at zero stress and the CB concentration in the PS phase (real CB concentration) is proposed regardless of the PS/PMMA ratio.

Keywords: Polymer-matrix composites; Modelling; Rheology

Received 12th March 2018, Accepted 2nd April 2018

DOI: 10.30919/es.180402

1. Introduction

The blending of polymers has been identified as one of the most convenient and economical methods to manufacture new multiphase polymeric materials that are able to meet the complex demands for performance.[1–3] Depending on the interactions between the ingredients, polymer blends can be classified into miscible, partially miscible and immiscible blends. In the case of immiscible polymer blends, two glass transition temperatures will be observed. Depending on the processing conditions and blend compositions, immiscible polymer blends can form various phase morphologies, such as sea-island, co-continuous, fibre and laminar, which have an important influence on the blend properties.[1–5] However, from the standpoint of a broader classification, immiscible polymer blends may be divided into two major categories: (1) one component forms a continuous phase and the other component forms a dispersed phase, showing a typical sea-island morphology; (2) the individual components each form continuous phases, giving rise to an interlocked or interpenetrated state of dispersion, showing a co-continuous morphology.

In general, a low volume fraction (minority) polymer component often forms a dispersed phase with a sea-island morphology. As the volume fraction of the minor phase increases to a critical concentration, the microstructure inverts from a sea-island morphology to a co-continuous morphology.[1–8] Aside from other parameters controlling morphology as thermal influence, the control of rheological parameters can influence the continuity in the matrix. Rheological experiments like oscillatory shear are frequently used to characterize the relationship between the rheology and the morphology of immiscible polymer blends.[6–13] In general, the rheological behaviour of immiscible polymer blends is characterized by an extra-contribution to the elastic moduli at low frequencies, corresponding to long-time relaxation process related to the presence of the interface. This increase in elasticity is shown in the plot of storage moduli vs. frequency as a shoulder for blends with sea-island morphology and as a power law for co-continuous morphology.[1]

Dynamic oscillatory experiments are more often used to characterize particle filled-polymers.[12–18] In nearly all cases the aim is to get some insight into the formation of a network of the particles added, which is indicated by the storage modulus vs. frequency. Much research has been done on the rheological behaviour of various conductive polymer composites and the comparison between the rheological threshold and the electrical percolation threshold.[19–27] However, from processing and application points of view, the rheological properties of polymer composites are very important. This property is related to the microstructure, the state of fillers' dispersion, the interactions between fillers and polymer chains. Therefore, it is interesting to study the rheological properties and correlate them with composites' properties.

[1] *National Engineering Research Center for Advanced Polymer Processing Technology, Zhengzhou University, Zhengzhou, 450002, China. E-mail: xianhu.liu@zzu.edu.cn*
[2] *Institute of Polymer Materials, Friedrich-Alexander University Erlangen-Nuremberg, Martensstr. 7, 91058 Erlangen, Germany. E-mail: xianhu.liu@zzu.edu.cn*
[3] *Department of Mechanical Engineering and Integrated Nanosystems Development Institute, Indiana University-Purdue University Indianapolis, 723 W. Michigan St, Indianapolis, IN 46202, USA*
[4] *Materials Engineering and Nanosensor [MEAN] Laboratory, Department of Chemical and Biological Engineering, The University of Alabama, Tuscaloosa, USA*

In this work, PMMA and PS were used as polymer matrix. The main advantage of these polymer matrices is high thermal stability, which allows investigations at elevated temperatures over long measuring time. On the other hand, PMMA is an optically clear (transparent) thermoplastic, and it is widely used as a substitute for inorganic glass, because it shows high impact strength, shatter-resistant, and exhibits favourable processing conditions; PS, as another most widely used plastics, is generally rigid and relatively inexpensive. Moreover, PMMA and PS are both amorphous thermoplastic polymers. Therefore, the influence of the crystallization on the distribution of the filler particles can be ignored. Accordingly, the rheological properties of PS/PMMA blend and their CB composites were systematically investigated.

2. Experimental section

2.1. Materials

Poly(methyl methacrylate) (PMMA) and polystyrene (PS) were used as the polymer matrix. Commercial PMMA Plexiglas 6N and PS 158N were provided by Evonik Röhm GmbH, Germany and Styrolution Group GmbH, Germany respectively. Material properties of PS and PMMA used in our work are summarized in Table 1. The carbon black used in this work was Printex® XE2 from Evonik industries. Printex® XE2 is conductive blacks with extraordinary electrical properties which differ significantly from those of conventional carbon blacks. This difference is essentially attributed to the porous structure of Printex® XE2. The specific surface area of the CB is about 886 m^2/g as measured by the Brunauer-Emmett-Teller (BET)-method and Dibutyl phthalate (DBP)-absorption is 380 ml/(100 g). The mean diameter of the primary particles is around 35 nm and the density at room temperature is 2.13 g/cm^3.

2.2. Composite preparation

All materials were dried at 80 °C in a vacuum oven for at least 18 h prior to processing. The PS/PMMA blends with different PS/PMMA ratio or PS/PMMA/CB composites filled with different CB concentrations from 0 to 6 vol.% were prepared by melt mixing in an internal mixer (Haake polyDrive 557-8310, Thermo Scientific, Germany) at 200 °C. Here, both polymers and CB were introduced directly into the mixer at a rotation speed of 20 rpm. After 2 min of mixing at 20 rpm, the rotational speed was increased to 60 rpm and kept constant for 8 min. After the melt mixing, the materials were cooled to room temperature and then granulated using a blade granulator (Wanner Technik). The granulate obtained was compression moulded in a hot press (Voigt) into 2 mm thick disks with a diameter of 25 mm. They were first preheated at 200 °C for 5 min under vacuum, and then pressed at 100 bar for 2 min before being cooled to room temperature for 10 min.

Table 1 Material properties of the PS and PMMA used in this study.

Polymer	T_g (°C)	Density (g/cm^3)	M_w (kg/mol)	M_w/M_n
PMMA	101	1.19	85	2.07
PS	105	1.05	268	2.50

2.3. Thermogravimetric analysis (TGA)

In order to determine the real volume fraction of the filler in the composite after sample preparation, thermal gravimetric analysis (TGA 2950, TA Instruments) was carried out. The procedures were as follows: the samples (ca. 20-30 mg) were heated from room temperature to 600 °C at a heating rate of 10 K/min under a nitrogen atmosphere.

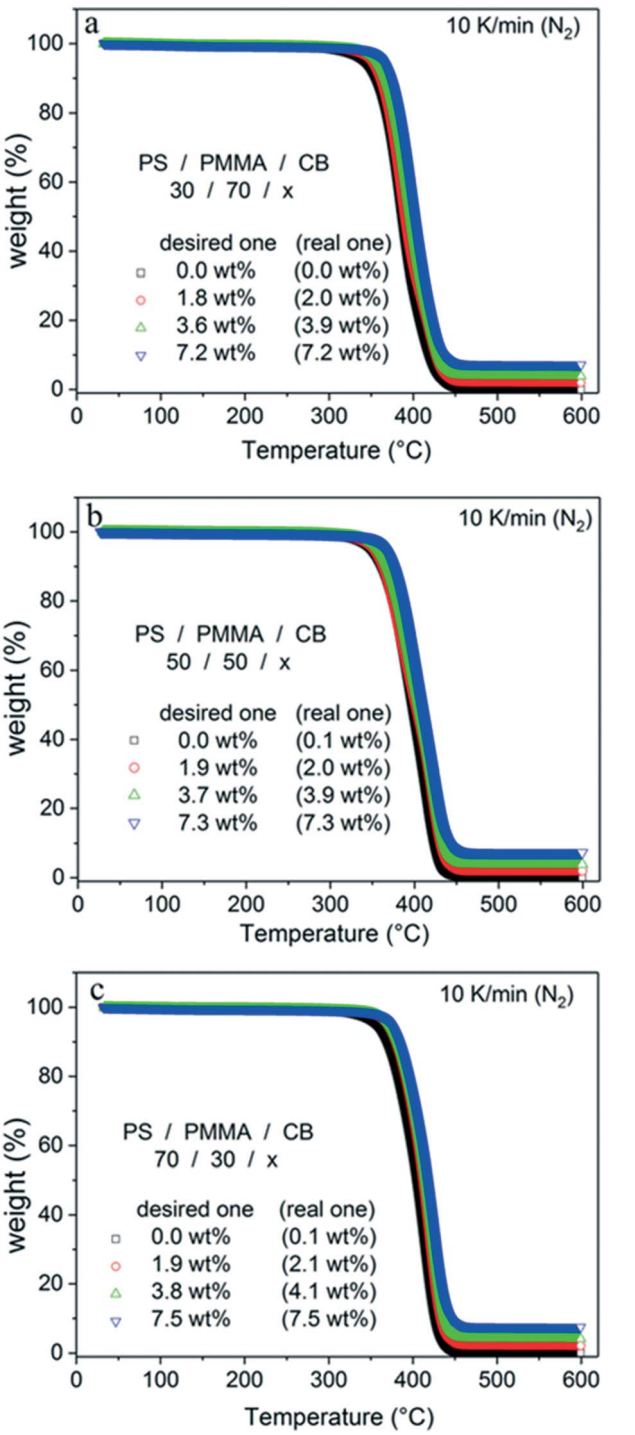

Fig. 1 TGA scans of PS/PMMA/CB composites. The samples were heated at 10 °C/min from 20 °C to 600 °C under N_2 atmosphere.

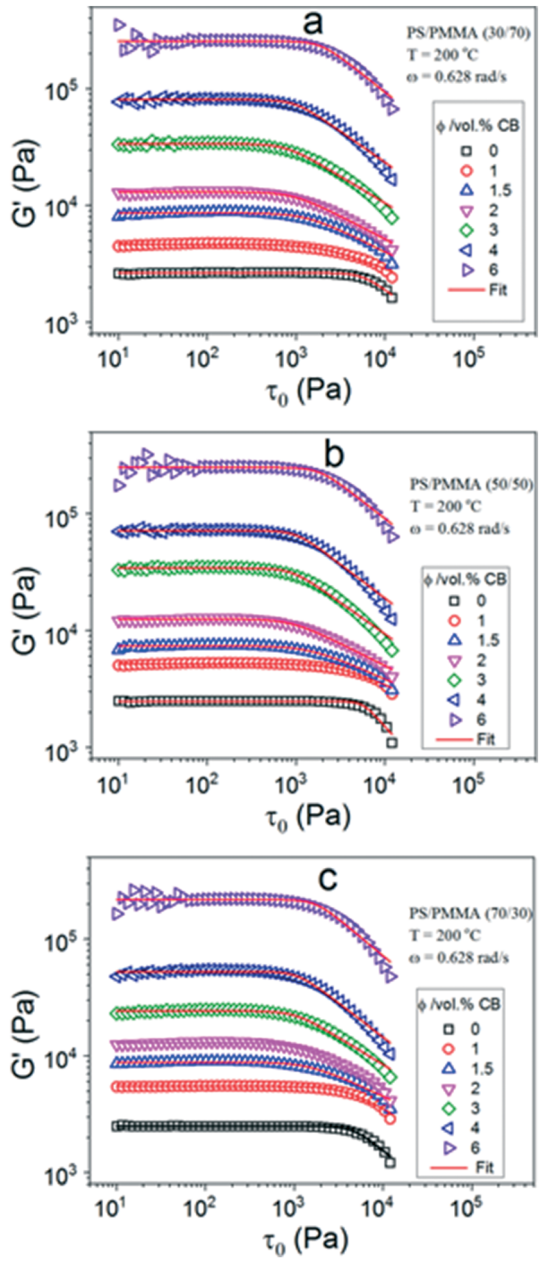

Fig. 2 Storage modulus as a function of stress amplitude of PS/PMMA/CB composites. Symbols are experimental data. Solid lines are fitting according to Eq. 1.

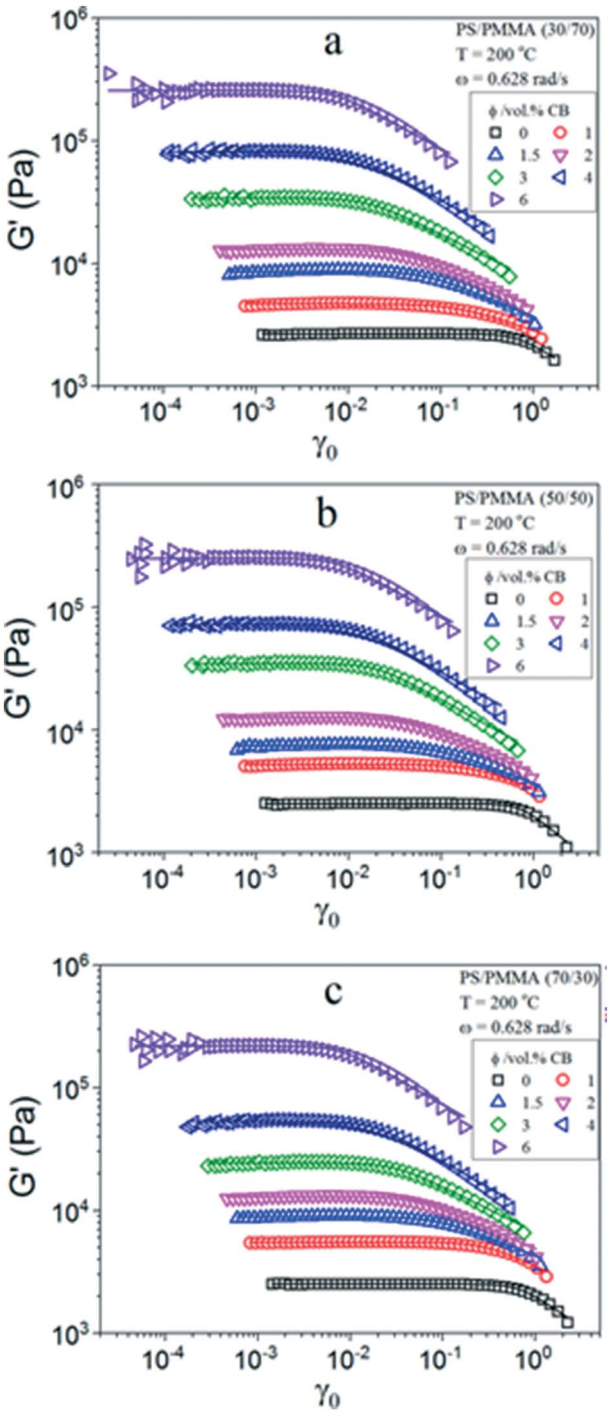

Fig. 3 Storage modulus as a function of deformation amplitude of PS/PMMA/CB composites. Symbols are experimental data. Solid lines are fittings according to Eq. 2.

2.4. Rheological measurements

Amplitude sweep tests were first performed to determine the linear viscoelastic region of the samples. The samples were exposed to an oscillatory shear stress, where the stress amplitude τ_0 was logarithmically increased and the angular frequency ω was kept constant. Time sweep tests at the constant angular frequency and constant amplitude were carried out to investigate the time-dependent rheological behaviour of the composites, as well as the thermal stability of the pure polymers and composites. Oscillatory frequency sweeps ranging from 0.01 to 100 rad/s were performed within the linear viscoelastic region of the samples. The storage modulus G', the loss modulus G'' and complex viscosity $|\eta^*|$ were recorded as functions of angular frequency.

3. Results and Discussion

The thermal decomposition of PS/PMMA/CB composites was investigated as a function of temperature under N_2 atmosphere. As shown in Fig. 1, the onset degradation temperature for all PS/

Table 2 Fit parameters determined by Eqs. 1 and 2 of amplitude sweeps for PS/PMMA/CB composites with different PS/PMMA ratio.

Ratio	ϕ/(vol. %)	$G'(0)$/Pa	τ_0^c/Pa	γ_0^c	$m_{\tau 0}$	$m_{\gamma 0}$
30/70	0	2663	5734	0.678	4.11	3.50
	1	4681	1979	0.154	2.10	1.90
	1.5	8629	1270	0.066	2.63	2.24
	2	13084	939	0.037	2.80	2.36
	3	33905	775	0.016	3.27	2.63
	4	81085	976	0.010	3.80	2.86
	6	255893	1874	0.007	4.27	2.96
50/50	0	2486	5762	0.710	6.31	4.39
	1	5214	2929	0.223	2.39	2.15
	1.5	7405	1405	0.089	2.38	2.09
	2	12587	894	0.040	2.73	2.31
	3	34446	894	0.019	3.85	2.93
	4	71872	1006	0.012	4.14	2.99
	6	249751	1824	0.007	4.24	2.94
70/30	0	2502	4617	0.664	4.40	3.69
	1	5506	3458	0.290	2.96	2.57
	1.5	8869	1452	0.088	2.49	2.15
	2	13014	1093	0.051	2.82	2.35
	3	24249	1035	0.030	3.32	2.63
	4	52785	1091	0.017	4.17	3.03
	6	218468	1746	0.008	4.55	3.05

PMMA/CB composites is higher than 300 °C. Therefore, the chosen processing temperature (200 °C) is below the thermal degradation temperature of all the compositions. On the other hand, no change in weight can be observed below 100 °C, suggesting that the drying process has removed the moisture of the samples. In addition, it is evident that the onset degradation temperature of the PS/PMMA/CB composites is larger than that of corresponding PS/PMMA blends, indicating the PS/PMMA/CB composites have better thermal stability in comparison with PS/PMMA blends. This enhancement may result from the interactions between organic and inorganic phase.[28] Furthermore, the real CB concentrations of the composites are close to the desired CB contents. As the deviations between the real and the desired CB concentration are very small, the values of the desired concentrations are used in this work.

In order to determine the linear-viscoelastic regime of PS/PMMA/CB composites, amplitude sweeps were carried out. The specimens were exposed to an oscillatory shear stress, where the stress amplitude τ_0 was logarithmically increased every 20 s from 10 Pa to 12 kPa and the angular frequency ω was kept constant ($\omega = 0.628$ *rad/s*).

Fig. 2 shows the storage modulus G' as a function of stress amplitude τ_0 for PS/PMMA/CB composites with different CB

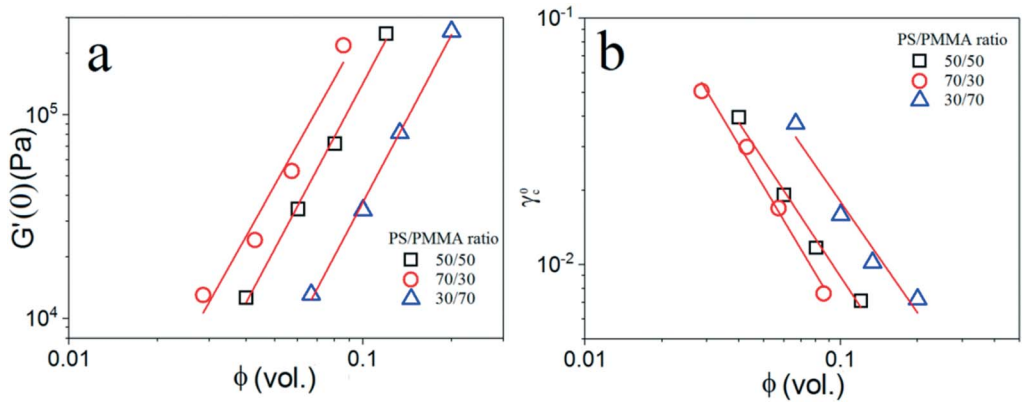

Fig. 4 The dependence of the storage modulus at zero stress $G'(0)$ (a) and critical strain (γ_0^c) (b) on the CB concentration in the PS phase (real CB concentration).

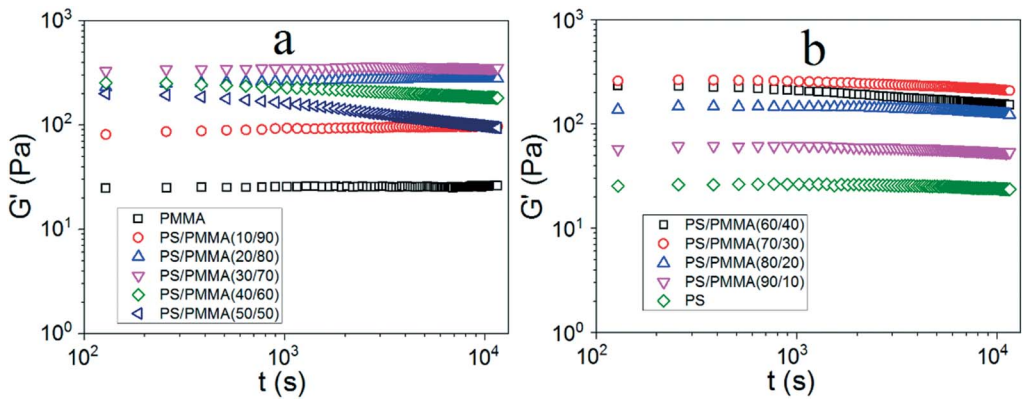

Fig. 5 G′ as a function of the residence time at 200 °C for PS/PMMA blends with different PS/PMMA ratio (ω = 0.05 rad/s, τ_0 = 200 Pa).

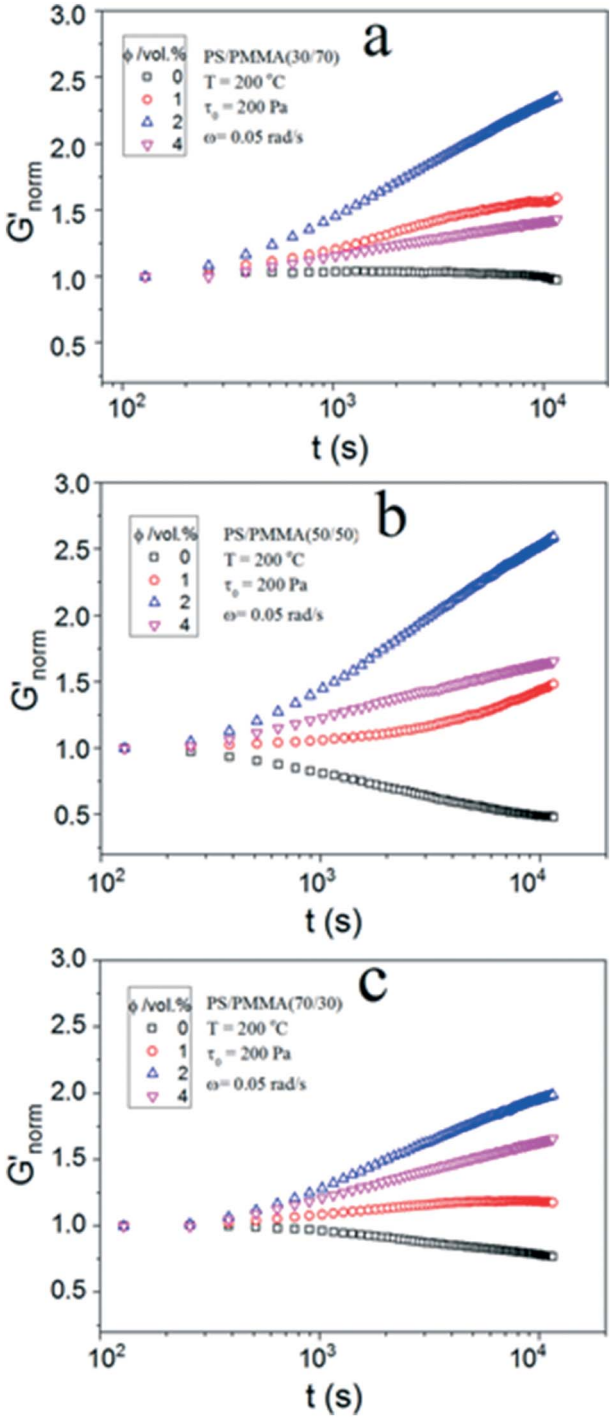

Fig. 6 Relative change of storage modulus as a function of the residence time at 200 °C for PS/PMMA blends with different CB concentration.

concentrations. As shown in Fig. 2, the signal of the storage modulus G' remains noisy at small stress amplitude for PS/PMMA/CB composites with high CB concentration, which is attributed to the insufficient resolution of the deformation signal. Furthermore, the elasticity (indicated by the storage modulus at zero stress $G'(0)$) of PS/PMMA/CB composites increases with increasing CB content. All the composites show yielding behaviour at a critical stress τ_0^c, at which $G'(0)$ decreases to 90% of its initial value. In this work, the stress amplitude of 200 Pa was chosen for the frequency and time sweep, which is in the linear region for all PS/PMMA/CB composites studied. Moreover, it is ensured that the measurements at 200 Pa provide sufficient resolution of the deformation signal.

In order to quantify the experimental data in detail, the following empirical equation was used to describe the experimental data[29,30]

$$G'(\tau_0) = G'(0)\left(1+\left(\frac{\tau_0}{\tau_0^c}\right)^{m_{\tau 0}}\right)^{-0.14} \quad (1)$$

where the parameter τ_0^c characterizes the stress amplitude at which the storage modulus at zero stress $G'(0)$ has decreased by about 10 %. As expected, Eq. 1 fits quite well for the experimental data.

The storage modulus G' as a function of strain amplitude γ_0 of PS/PMMA/CB composites with different CB concentrations was also given, as shown in Fig. 3. A similar approach can analogously be used to describe the data:

$$G'(\gamma_0) = G'(0)\left(1+\left(\frac{\gamma_0}{\gamma_0^c}\right)^{m_{\gamma 0}}\right)^{-0.14} \quad (2)$$

where the parameter γ_0^c characterizes the strain amplitude at which the storage modulus at zero stress $G'(0)$ has decreased by about 10 %. The results of the fit parameters can be found in Table 2. As can be seen, as the CB concentration increases, the τ_0^c first decreases and then increases, which is in agreement with that of PMMA/CB composites, as reported by Krückel et al.[31] At lower CB concentration range, the effect of polymer-filler interactions becomes dominant. Destruction of the polymer-filler interaction, i.e. detachment of the polymer chains from the particle surfaces, requires smaller stress amplitude, compared to those necessary for chain disentanglement. At higher CB concentration, the filler-filler interaction and the filler network become the dominant effect, and higher stress amplitude is required for the breakdown of the filler network, leading to a higher τ_0^c. Furthermore, the γ_0^c decreases with increasing the CB concentration due to the more polymer-filler interactions or more filler-filler network.

The elastic properties of the PS/PMMA/CB composites can also be evaluated using fractal scaling theories developed for colloidal gels. Particles flocculate in a dispersion medium, and a continuous network of particles is formed throughout the medium in colloidal gels. Shih et al. developed a scaling theory that correlates the volume fraction of the particles to the critical strain (γ_0^c) and the elastic modulus ($G'(0)$) of the flocculated gels.[32] At relatively low particle concentrations, the interactions between neighbouring flocs are thought to be higher than those within the flocs (i.e., in the "strong-link regime"), and the following scaling relationships hold:[33,34]

$$G'(0) \propto \phi^{(3+x)/(3-d_f)} \quad (3)$$

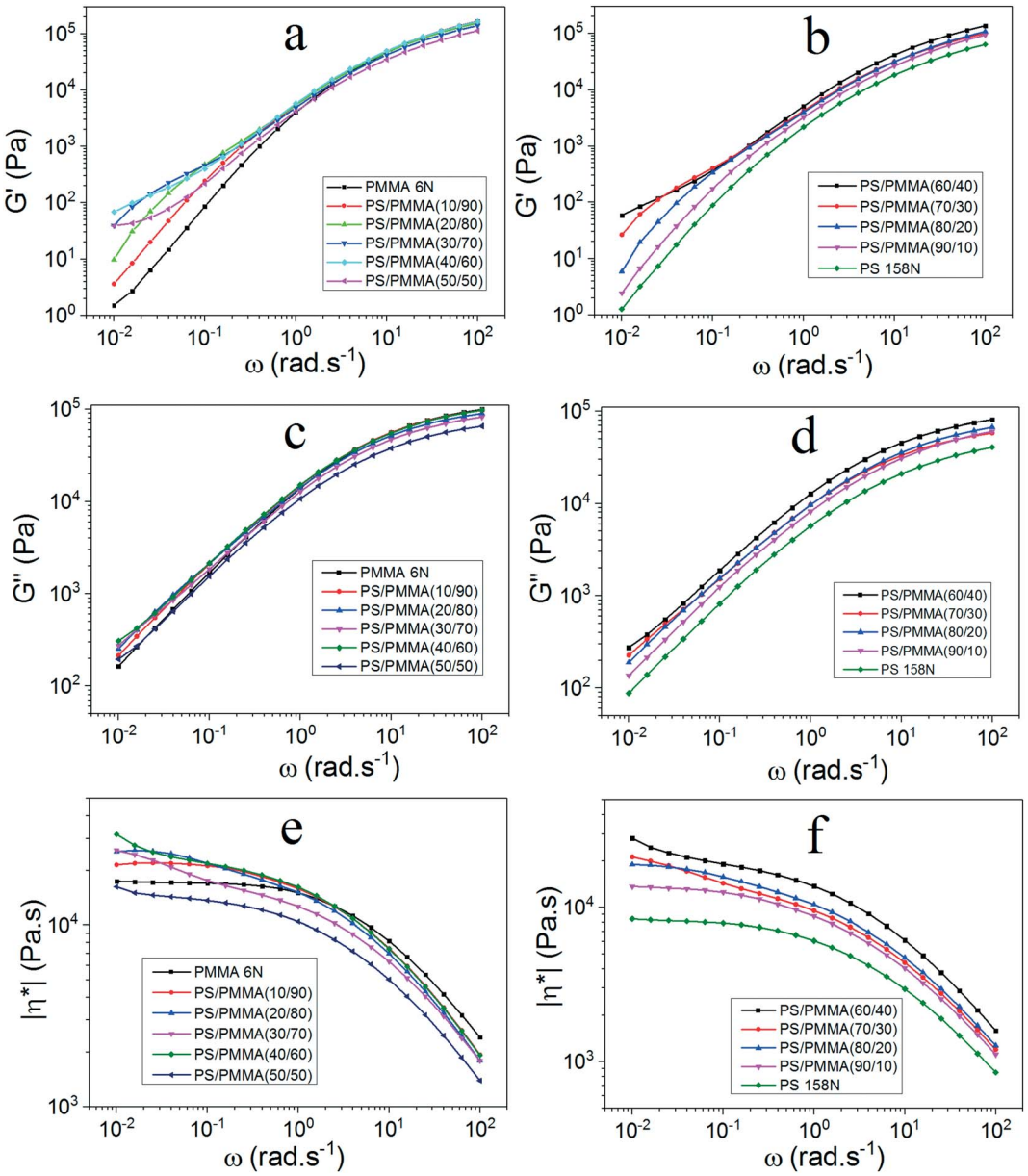

Fig. 7 Storage modulus (G′), loss modulus (G″) and magnitude of complex viscosity ($|\eta^*|$) as a function of angular frequency ω for PS/PMMA blends with different PS/PMMA ratios.

$$\gamma_0^c \propto \phi^{-(1+x)/(3-d_f)} \tag{4}$$

where x is the backbone fractal dimension of the flocs and d_f is the fractal dimension of the flocs. These two scaling equations were used to fit the storage moduli and the critical strains in Fig. 4. The PS/PMMA/CB composites show the scaling relationship $G'(0) \propto \phi^{2.7}$, and $\gamma_0^c \propto \phi^{-1.5}$. Based on the obtained exponents, d_f = 1.33 and x = 1.5, which are similar to the literature.[35]

When long measuring time and high temperatures are applied, a precondition for reliable rheological measurements is the thermal stability of the material. A very common way to evaluate the thermal stability of samples in the molten state is to measure the storage modulus G′ as a function of time at a defined temperature in the terminal region. Fig. 5 shows the thermal stability tests of PS/PMMA blends with different PS/PMMA ratio at the processing temperature 200 °C and at a small angular frequency of 0.05 rad/s and a linear shear stress of 200 Pa. As can be seen from Fig. 5, the storage modulus of the PMMA and PS matrices remain constant over time. A distinct thermal degradation is not observed at this temperature within even 10 000 s of measuring time. This indicates that the PMMA and PS have a good thermal stability. However, for PS/PMMA blends with PS/PMMA ratio of 40/60, 50/50, 60/40, 30/70 and 70/30, G′ decreases in the early stages; afterward, they decrease slowly and moderately and eventually approach equilibrium. In more detail, the apparent reduced G′ in the early stage can be attributed to the coupling effects of the reduced concentration fluctuations and

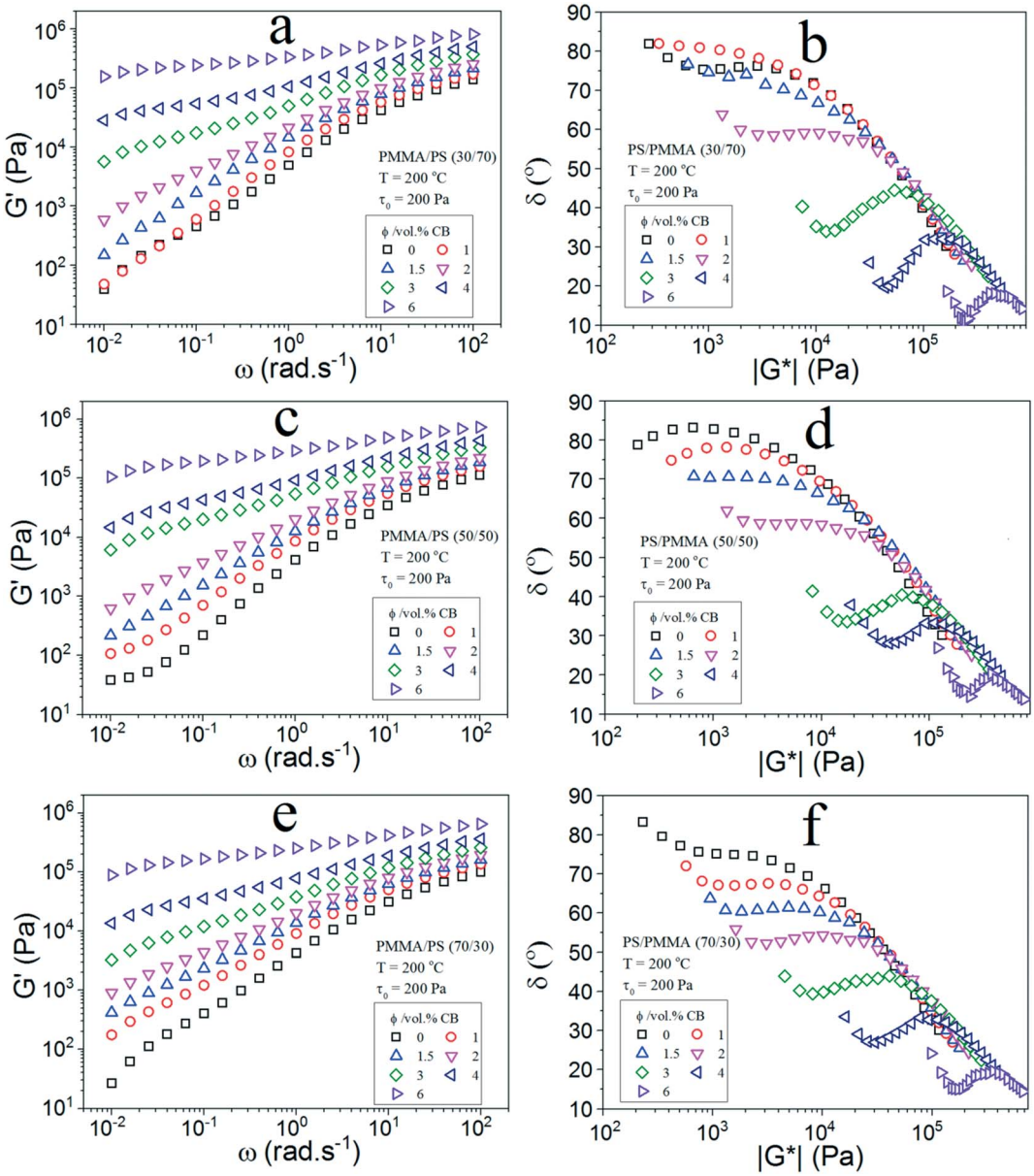

Fig. 8 Storage modulus (G′) as a function of frequency (ω) (a, c, e) and the van Gurp-Palmen plot (b, d, f) for PS/PMMA/CB composites with PS/PMMA ratio of (a, b) (30/70), (c, d) (50/50) and (e, f) (70/30).

decreased interfacial area due to interfacial tension-driven dispersed phase coarsening and coalescence. In the late stages, when the concentration fluctuations and interfacial area become nearly saturated, G′ of the PS/PMMA composites weakly decreases.[36–38]

The time-dependent behaviour of G′ for the PS/PMMA/CB can differ from the unfilled PS/PMMA blends due to interactions between CB particles and polymer. Therefore, the time-dependent behaviour of G′for the PS/PMMA/CB composites with different CB concentration was investigated by means of the time sweep tests. Fig. 6 shows the time-dependent behaviour of G′ for the PS/PMMA/CB composites with PS/PMMA ratio of 30/70, 50/50 and 70/30 under time sweeps at a small angular frequency of 0.05 rad/s and a linear shear stress of 200 Pa. As can be seen from Fig. 6, G′ of the PS/PMMA/CB composites is not constant over time. G′ increases with the measuring time for all PS/PMMA/CB composites. Similar rheological behavior had been observed in CNT-filled polymer composites. The majority of the explanations given in the literature interpret the time-dependent increase of storage modulus as a consequence of the aggregation of particles to a higher structure.[39–42] Moreover, increasing the CB concentration above the percolated CB concentrations, the changes in the time-dependent behaviour of storage modulus decreases for all materials investigated.

Fig. 7 shows the dynamic moduli for the PS/PMMA blends with different ratios. As predicted, G' deviates from the typical terminal behavior $[G'(\omega \rightarrow 0) \sim \omega^2]$ for all polymer blends. For the blends (20/80, 30/70, 70/30 and 80/20), a shoulder is seen at low-frequency region due to the shape relaxation of dispersed droplets, indicating the formation of a typical sea-island structure. However,

the 50/50 blend exhibits power-law dependences with small terminal slope, and which is characteristic for co-continuous structure.[1]

As the selective localization of the particles affects the phase morphology evidently, it may influence the final performance of the composites. Therefore, the rheological behavior was characterized and the dynamic storage modulus G' obtained from the dynamic frequency sweep is shown in Fig. 8. It is notable that the storage modulus increases significantly at low angular frequencies ω due to the incorporation of CB. The subsequent enhancement in modulus with increasing CB concentration is due to the confinement effect and interaction between polymer and filler. As the CB concentration increases, the slope of $logG'$ versus $log\omega$ plots in the low angular frequencies for the composites becomes much lower than 1 (3 vol.% CB). This suggests that the composite exhibits a transformation from liquid-like to solid-like states due to filler-polymer or filler-filler network formation.[43] The van Gurp-Palmen plot is usually used to estimate the rheological percolation of the composites.[44–47] Figure 8b, d, f shows the van Gurp-Palmen plots of phase angle δ versus complex modulus $|G^*|$for the PS/PMMA/CB systems. The low-frequency δ of the unfilled PS/PMMA is close to 80°, which is indicative of a flow behavior presented by the viscoelastic fluid. With the addition of CB particles, the low-frequency δ of the composites decreases. When the CB loading is increased to 3 vol.%, the low-frequency δ decreases remarkably to lower than 45°, indicating a rheological liquid-solid transition in that composite system. Accordingly, the rheological percolation threshold for the PS/PMMA/CB systems is between 2 and 3 vol.% CB.

4. Conclusions

This work focuses on the rheological behavior of CB-filled immiscible PS/PMMA blends in order to explore the influence of phase morphology and CB concentration on the rheological properties. The amplitude sweeps were first carried out to determine the linear-viscoelastic regime. The oscillatory frequency sweep was used to characterize CB network and the phase morphology of immiscible polymer blends. Due to the shape relaxation of dispersed droplets, a shoulder at low-frequency region is found for the blends with a sea-island morphology; while the blend with a co-continuous morphology exhibits power-law dependences with a small terminal slope during the frequency sweep. As the CB concentration increases, the slope of $logG'$ versus $log\omega$ plots in the low angular frequencies for the composites becomes much lower than 1 (3 vol.% CB), indicating a transformation from liquid-like to solid-like states. In addition, the storage moduli at zero stress and the real CB concentration shows a linear relationship regardless of the PS/PMMA ratio.

Conflict of interest

The authors declare that they have no conflict of interest.

References

1 C. R. López-Barrón and C. W. Macosko, *J. Rheol.*, 2012, **56**, 1315.
2 F. Goharpey, H. Nazockdast and A. A. Katbab, *Polym. Eng. Sci.*, 2005, **45**, 84.
3 N. C. Das, H. Wang, J. Mewis and P. Moldenaers, *J. Polym. Sci. Polym. Phys.*, 2005, **43**, 3519.
4 M. Castro, C. Carrot and F. Prochazka, *Polymer*, 2004, **45**, 4095.
5 I. Vinckier, P. Moldenaers and J. Mewis, *Rheol. Acta.*, 1999, **38**, 65.
6 J. Wang and S. Velankar, *Rheol. Acta*, 2006, **45**, 297.
7 I. Vinckier, P. Moldenaers and J. Mewis, *J. Rheol.*, 1996, **40**, 613.
8 W. Yu, W. Zhou and C. Zhou, *Polymer*, 2010, **51**, 2091.
9 Y. Pan, X. Liu, X. Hao and D. W. Schubert, *Phys. Chem. Chem. Phys.*, 2016, **18**, 32125.
10 Y. Pan, X. Liu, J. Kaschta, C. Liu and D. W. Schubert, *J. Rheol.*, 2017, **61**, 759.
11 Y. Pan, X. Liu, X. Hao, Z. Starý and D. W. Schubert, *Eur. Polym. J.*, 2016, **78**, 106.
12 X. Liu, Y. Pan, G. Zheng and D. W. Schubert, *Compos. Sci. Technol.*, 2016, **128**, 1.
13 Y. Pan, X. Liu, J. Kaschta, X. Hao, C. Liu and D. W. Schubert, *Polymer*, 2017, **113**, 34.
14 Z. Lu, Y. Pan, X. Liu, G. Zheng, D. W Schubert and C. Liu, *Mater. Lett.*, 2018, **221**, 62.
15 X. Liu, J. Krückel, G. Zheng and D. W. Schubert, *ACS Appl. Mater. Interfaces*, 2013, **5**, 8857.
16 X. Hao, J. Kaschta, Y. Pan, X. Liu and D. W. Schubert, *Polymer*, 2016, **82**, 57.
17 X. Liu, J. Krückel, G. Zheng and D. W. Schubert, *Compos. Sci. Technol.*, 2014, **100**, 99.
18 P. Chu, H. Zhang, F. Chen and Z. Zhang, *Compos. Part A-Appl. S.*, 2016, **81**, 34.
19 F. Du, R. C. Scogna, W. Zhou, S. Brand, J. E. Fischer and K. I. Winey, *Macromolecules*, 2004, **37**, 9048.
20 M. Sabzi, L. Jiang, F. Liu, I. Ghasemi and M. Atai, *J. Mater. Chem. A*, 2013, **1**, 8253.
21 K. Kota, B. H. Cipriano, D. Powell, S. R. Raghavan and H. A. Bruck, *Nanotechnology*, 2007, **18**, 505705.
22 G. Wu, J. Lin, Q. Zheng and M. Zhang, *Polymer*, 2006, **47**, 2442.
23 D. S. Bangarusampath, H. Ruckdäschel, V. Altstädt, J. K. Sandler, D. Garray and M. S. Shaffer, *Chem. Phys. Lett.*, 2009, **482**, 105.
24 C. Gao, S. Zhang, F. Wang, B. Wen, C. Han, Y. Ding and M. Yang, *ACS Appl Mater Interfaces*, 2014, **6**, 12252.
25 D. Ren, S. Zheng, F. Wu, W. Yang, Z. Liu and M. Yang, *J. Appl. Polym. Sci.*, 2014, **131**, 39953.
26 G. Hu, C. Zhao, S. Zhang, M. Yang and Z. Wang, *Polymer*, 2006, **47**, 480.
27 Y. Pan and L. Li, *Polymer*, 2013, **54**, 1218.
28 X. Fu and S. Qutubuddin, *Polymer*, 2001, **42**, 807.
29 P. Cassagnau, *Polymer*, 2003, **44**, 2455.
30 A. Das, K. W. Stoeckelhuber, R. Jurk, M. Saphiannikova, J. Fritzsche, H. Lorenz, M. Klueppel and G Heinrich, *Polymer*, 2008, **49**, 5276.
31 J. Krückel, PhD thesis, University Erlangen-Nürnberg, 2015.
32 W. H. Shih, W. Y. Shih, S. I. Kim, J. Liu and I. A. Aksay, *Phys. Rev. A*, 1990, **42**, 4772.
33 J. M. Piau, M. Dorget and J. F. Palierne, *J. Rheol.*, 1990, **43**, 305.
34 T. Chatterjee and R. Krishnamoorti, *Phys. Rev. E*, 2007, **75**, 050403.
35 G. Heinrich and M. Klüppel, *Recent advances in the theory of filler networking in elastomers*, Springer, Berlin Heidelberg, 2002.
36 M. Kapnistos, A. Hinrichs, D. Vlassopoulos, S. H. Anastasiadis, A. Stammer and B. A. Wolf, *Macromolecules*, 1996, **29**, 7155.

37 I. Vinckier and H. M. Laun, *Rheol. Acta*, 1999, **38**, 274.
38 Y. H. Niu and Z. G. Wang, *Macromolecules*, 2006, **39**, 4175.
39 R. Haggenmueller, J. E. Fischer and K. I. Winey, *Macromolecules*, 2006, **39**, 2964.
40 P. Pötschke, M. Abdel-Goad, I. Alig, S. Dudkin and D. Lellinger, *Polymer*, 2004, **45**, 8863.
41 L. Karasek and M. Sumita, *J. Mater. Sci.*, 1996, **31**, 281.
42 Y. Song, C. Xu and Q. Zheng, *Soft Matter*, 2004, **10**, 2685.
43 J. Ren, A. S. Silva and R. Krishnamoorti, *Macromolecules*, 2000, **33**, 3739.
44 K. Kota, B. H. Cipriano, M. K. Duesterberg, A. L. Gershon, D. Powell, S. R. Raghavan and H. A. Bruck, *Macromolecules*, 2007, **40**, 7400.
45 X. F. Wei, R. Y. Bao, Z. Q. Cao, W. Yang, B. H. Xie and M. B. Yang, *Macromolecules*, 2014, **47**, 1439.
46 J. Zhu, S. Wei, Y. Li, L. Sun, N. Haldolaarachchige, D. P. Young, C. Southworth and A. Khasanov, *Macromolecules*, 2011, **44**, 4382.
47 X. Zhang, X. Yan, Q. He, H. Wei, J. Long, J. Guo, H. Gu, J. Yu and Z. Guo, *ACS Appl. Mater. Interfaces*, 2015, **7**, 6125.

